Supplementary Figure 1. A) Growth of integrated Ulp2 C-terminal mutations on YPD at 30 °C. B) Cell growth of WT, *ulp2-SIM*^{3A}*CCR*^{3A}*F839D*, *ulp2-SIM*^{PIASX}*CCR*^{3A}*F839D* and *ulp2-SIM*$^{M\text{-}IR2}$*CCR*^{3A}*F839D* on indicated growth media at 30 °C.

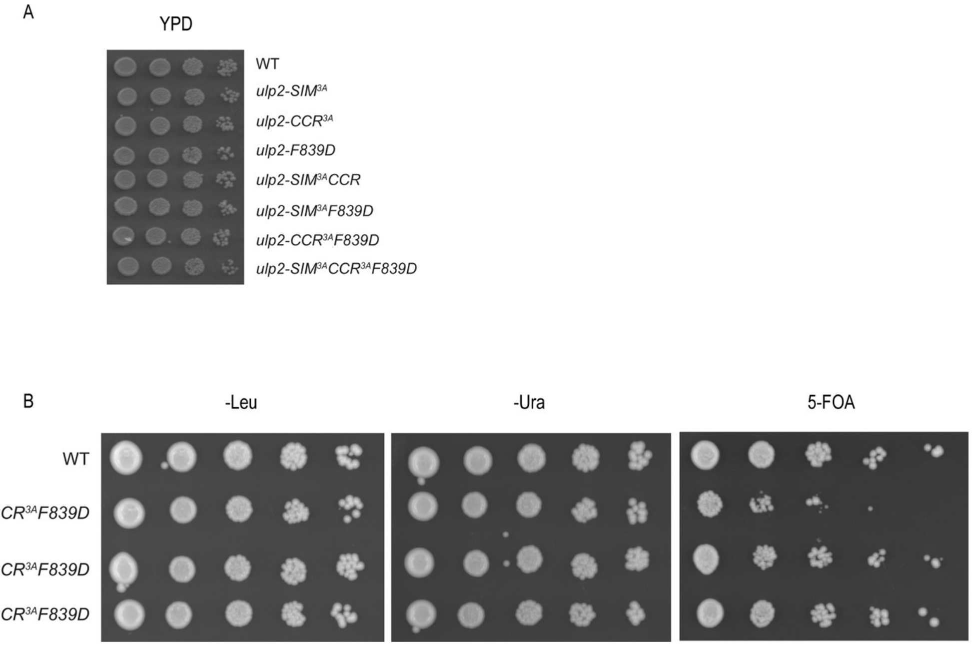

Supplementary Figure 2. A) Abundance of TAF tagged Ulp2 in the HF-SUMO strains used for quantitative MS analysis. Coomassie staining is shown as a loading control. B) Asynchronous cell cycle profiles of the *ulp2* mutants that were used for quantitative MS analysis. WT is also included for reference.

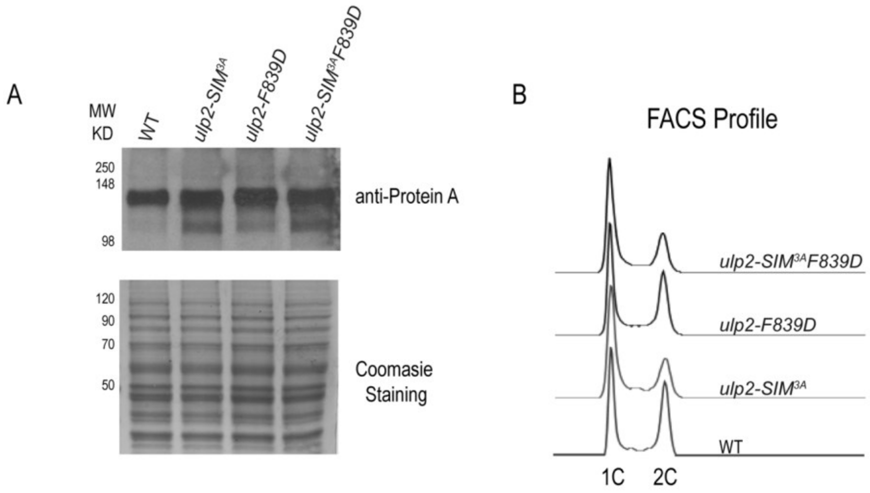

Supplementary Table 1. The average of the abundance ratios of the peptides derived from sumoylated Cdc14, Net1 and Tof2 in various *ulp2* mutants were calculated along with their standard deviations. The fold increase of sumoylated Tof2 is less pronounced than those of Net1 and Cdc14, and is due to an overall decrease in Tof2 abundance; which is dependent on poly-SUMO formation (21,29).

Protein	*ulp2-SIM*^{3A} */ WT*	*ulp2-F839D / WT*	*ulp2-SIM*^{3A} *F839D / WT*
Cdc14	17.7 ± 9.3	9.6 ± 2.5	31.7 ± 12.5
Net1	10.6 ± 0.6	5.1 ± 0.6	18.7 ± 1.7
Tof2	4.8 ± 0.6	1.5 ± 0.4	5.9 ± 1.3

Supplementary Table 2. Yeast strains and plasmids used in this study

STRAIN NAME	GENOTYPE	SOURCE
HZY3658	MAT a, *ulp2Δ::natMX4*, pRS316-*ULP2,* W303	This study
HZY2101	MAT a, *HF-SMT3 sml1Δ::TRP1 arg4Δ ura3-52 leu2Δ1 trp1Δ63 his3Δ200 lys2ΔBgl hom3-10 ade2Δ ade8.*	Albuquerque, et al, PLoS genetics 2013
HZY3676	MAT a, *NET1-HH::HIS3 HF-SMT3,* isogenic to HZY2101	This study
HZY3678	MAT a, *NET1-HH::HIS3 ulp2-SIM*^{3A}*::kanMX6 HF-SMT3,* derived from HZY3676	This study
HZY3679	MAT a, *NET1-HH::HIS3 ulp2-F839D:: kanMX6 HF-SMT3,* derived from HZY3676	This study
HZY3680	MAT a, *NET1-HH::HIS3 ulp2-SIM*^{3A}*F839D:: kanMX6, HF-SMT3,* derived from HZY3676	This study
HZY3973	MAT a, *Ulp2-TAF:: kanMX6 HF-SMT3,* derived from HZY2101	This study
HZY3963	MAT a, *ulp2-SIM*^{3A}*-TAF:: kanMX6 HF-SMT3,* derived from HZY2101	This study
HZY3966	MAT a, *ulp2-F839D-TAF:: kanMX6 HF-SMT3,* derived from HZY2101	This study
HZY3983	MAT a, *ulp2-SIM*^{3A}*F839D-TAF:: kanMX6 HF-SMT3,* derived from HZY2101	This study

HZY621	MAT**a**; *RDN1-NTS1::mURA3 ade2-1 can1-100 his3-11,15 leu2-3,112 trp1-1 ura3-1 RAD5+ cir0(2μm removed), also known as JLY1096*	Liang et al. Genes & Dev. 2017
HZY001	*ulp2-SIM*^{3A}*::kanMX6, derived from HZY621*	This study
HZY002	*ulp2-CCR*^{3A}*::kanMX6, derived from HZY621*	This study
HZY035	*ulp2-F839D::kanMX6, derived from HZY621*	This study
HZY003	*ulp2-SIM*^{3A}*, F839D::kanMX6, derived from HZY621*	This study
HZY004	*ulp2-F839D, CCR*^{3A}*::kanMX6, derived from HZY621*	This study
HZY005	*ulp2-SIM*^{3A}*, CCR*^{3A}*::kanMX6, derived from HZY621*	This study
HZY006	*ulp2-SIM*^{3A}*, F839D, CCR*^{3A}*::kanMX6, derived from HZY621*	This study

PLASMID	DESCRIPTION	SOURCE
HZE2340	pRS315-Ulp2-TAF:: *kanMX6*	This study
HZE2341	pRS315-*ulp2-SIM*^{3A}-TAF:: *kanMX6*	This study
HZE2342	pRS315-*ulp2-F839D*-TAF:: *kanMX6*	This study
HZE2527	pRS315-*ulp2-CCR*^{3A}-TAF:: *kanMX6*	This study
HZE2343	pRS315-*ulp2-(SIM*^{3A}*, F839D)*-TAF:: *kanMX6*	This study
HZE2525	pRS315-*ulp2-(SIM*^{3A}*, CCR*^{3A}*)*-TAF:: *kanMX6*	This study
HZE2526	pRS315-*ulp2-(F839D, CCR*^{3A}*)*-TAF:: *kanMX6*	This study
HZE2439	pRS315-*ulp2-(SIM*^{3A}*, F839D, CCR*^{3A}*)*-TAF:: *kanMX6*	This study
HZE1145	LIC-2BT-Ulp2-(400-767)	This study
HZE1142	LIC-2BT-*ulp2-SIM*^{3A}-(400-767)	This study
HZE2346	Lic-2BT-Smt3 (1xSUMO)	This study
HZE2347	LIC-2BT-2xSmt3 (2xSUMO)	This study
HZE2348	LIC-2BT-4xSmt3 (4xSUMO)	This study
HZE2349	LIC-2BT-6xSmt3 (6xSUMO)	This study
HZE2585	pRS315-*ulp2 (PIASX-SIM, F839D, CCR*^{3A}*)*-TAF:: *kanMX6,* Ulp2-SIM (sequence IQII) is substituted by PIASX-SIM (sequence: VDVIDL)	This Study
HZE2586	pRS315-*ulp2 (M-IR2-SIM, F839D, CCR*^{3A}*)*-TAF:: *kanMX6.* Ulp2-SIM (sequence IQII) is substituted by RanGAP M-IR2-SIM (sequence: VIIVW)	This Study

- *HF-SMT3* refers *to 6xHIS-3xFLAG-SMT3*. HH tag refers to 6xHIS-3xHA tag. TAF refers to 6xHIS-3xFLAG-Protein A.

- Lic-2BT plasmid contains N-terminal 6xHIS and a TEV protease cleavage site sequence.

Supplementary Table 3. The median abundance ratios of the peptides derived from the SILAC SUMO proteomic experiment comparing HZY3963 (light media) and HZY 2101 (heavy media). A minimum requirement of 5 peptides IDs was used to filter the results.

Light: HZY3963 Heavy: HZY2101				
ORF	Gene	Median Ratio	Log$_2$(Mutant/WT)	# of Peptide IDs
YLR314C	CDC3	0.70	-0.52	25
YJR076C	CDC11	0.68	-0.56	6
YDL225W	SHS1	0.67	-0.58	15
YJR092W	BUD4	0.54	-0.89	6
YKR095W	MLP1	0.85	-0.23	42
YIL149C	MLP2	0.87	-0.20	38
YJL041W	NSP1	0.36	-1.48	7
YLR335W	NUP2	0.29	-1.78	15
YOR341W	RPA190	1.20	0.26	17
YOR340C	RPA43	1.72	0.79	8
YBR049C	REB1	0.74	-0.44	26
YJL140W	RPB4	0.39	-1.34	10
YDL140C	RPO21	0.98	-0.02	48
YOR194C	TOA1	0.48	-1.06	5
YBR279W	PAF1	0.34	-1.57	13
YPR133C	SPN1	0.37	-1.42	7
YML010W	SPT5	0.51	-0.98	40
YER148W	SPT15	2.47	1.31	7
YGR186W	TFG1	0.56	-0.84	34
YLR399C	BDF1	0.49	-1.03	20
YGR252W	GCN5	0.57	-0.81	16
YGL066W	SGF73	0.58	-0.79	7
YBR081C	SPT7	0.58	-0.77	42
YKR025W	RPC37	0.40	-1.34	12
YDL150W	RPC53	0.79	-0.35	16
YPR190C	RPC82	0.64	-0.64	27
YOR207C	RET1	0.51	-0.97	17
YAL001C	TFC3	0.81	-0.30	39
YNL039W	BDP1	1.04	0.06	21
YDR362C	TFC6	0.39	-1.35	6
YOR110W	TFC7	0.80	-0.33	11

YGR246C	BRF1	0.81	-0.31	24
YOR113W	AZF1	0.61	-0.70	10
YOR028C	CIN5	0.50	-1.01	9
YCR084C	TUP1	0.46	-1.12	41
YBR112C	CYC8	0.48	-1.05	17
YNL167C	SKO1	0.43	-1.21	23
YPL181W	CTI6	0.42	-1.24	13
YNL027W	CRZ1	0.68	-0.55	10
YPL049C	DIG1	0.41	-1.29	5
YHR084W	STE12	0.44	-1.18	9
YBR083W	TEC1	0.87	-0.20	12
YNL199C	GCR2	0.27	-1.88	5
YLR256W	HAP1	1.00	0.00	7
YNL103W	MET4	0.49	-1.03	16
YDR176W	NGG1	0.48	-1.05	12
YDR310C	SUM1	0.59	-0.77	57
YER111C	SWI4	0.70	-0.52	15
YOR344C	TYE7	2.21	1.15	8
YDR213W	UPC2	0.54	-0.89	16
YIL056W	VHR1	0.63	-0.67	7
YER064C	YER064C	1.94	0.96	10
YPL228W	CET1	0.30	-1.76	25
YAL032C	PRP45	0.72	-0.48	7
YMR229C	RRP5	1.25	0.32	7
YDR464W	SPP41	1.04	0.05	86
YDR169C	STB3	0.84	-0.25	14
YOR038C	HIR2	0.38	-1.39	20
YBR215W	HPC2	0.38	-1.39	23
YDR174W	HMO1	1.13	0.18	6
YBR245C	ISW1	0.55	-0.86	34
YML069W	POB3	0.49	-1.04	18
YOL004W	SIN3	0.63	-0.67	19
YDR359C	VID21	0.47	-1.10	24
YGR056W	RSC1	0.48	-1.07	23
YLR357W	RSC2	0.57	-0.81	50
YFR037C	RSC8	0.43	-1.20	22
YLR033W	RSC58	0.48	-1.06	18
YMR091C	NPL6	0.74	-0.43	7
YIL126W	STH1	0.64	-0.64	33
YDR190C	RVB1	0.39	-1.34	9
YOR290C	SNF2	0.79	-0.33	23

YBR289W	SNF5	0.66	-0.59	9
YJL176C	SWI3	0.64	-0.63	18
YDR334W	SWR1	0.61	-0.72	35
YAL011W	SWC3	0.43	-1.21	20
YDR485C	VPS72	0.52	-0.96	36
YDL197C	ASF2	0.64	-0.65	8
YKL172W	EBP2	0.91	-0.13	7
YDR110W	FOB1	2.31	1.21	20
YFR028C	CDC14	20.07	4.33	20
YJL076W	NET1	10.64	3.41	138
YNL216W	RAP1	0.60	-0.73	34
YLR442C	SIR3	0.93	-0.11	22
YDR227W	SIR4	0.74	-0.43	65
YKR010C	TOF2	4.43	2.15	29
YFL008W	SMC1	1.00	0.00	11
YJL074C	SMC3	1.40	0.49	13
YDL003W	MCD1	2.26	1.17	12
YFR031C	SMC2	1.50	0.58	24
YLR086W	SMC4	1.08	0.11	41
YBL097W	BRN1	0.94	-0.08	20
YOL034W	SMC5	1.04	0.06	16
YLR383W	SMC6	0.91	-0.14	8
YJR089W	BIR1	0.69	-0.53	53
YGR140W	CBF2	1.56	0.64	28
YBR156C	SLI15	0.42	-1.26	26
YKL112W	ABF1	0.58	-0.78	30
YLL004W	ORC3	0.88	-0.19	7
YBR088C	POL30	0.67	-0.57	14
YOL006C	TOP1	1.47	0.56	27
YNL088W	TOP2	1.14	0.19	34
YAL027W	YAL027W	0.73	-0.44	5
YBR114W	RAD16	0.55	-0.86	17
YPR180W	AOS1	0.77	-0.39	7
YDR390C	UBA2	1.09	0.13	15
YDL064W	UBC9	0.39	-1.35	7
YDR409W	SIZ1	0.54	-0.88	18
YOR156C	NFI1	1.17	0.23	7
YNL042W	BOP3	1.07	0.09	12
YDL126C	CDC48	4.75	2.25	43
YDR385W	EFT2	1.71	0.77	11
YGR254W	ENO1	5.84	2.55	15

YKL142W	MRP8	0.93	-0.10	5
YLR044C	PDC1	2.22	1.15	16
YCR012W	PGK1	1.83	0.87	25
YOR191W	RIS1	1.27	0.34	18
YJL138C	TIF2	0.83	-0.27	13
YMR111C	YMR111C	1.13	0.18	32
YBL023C	MCM2	2.74	1.45	7
YEL032W	MCM3	5.73	2.52	12

Supplementary Table 4. The median abundance ratios of the peptides derived from the SILAC SUMO proteomic experiment comparing HZY3966 (light media) and HZY 2101 (heavy media). A minimum requirement of 5 peptides IDs was used to filter the results.

Light: HZY3966 Heavy: HZY2101				
ORF	Gene	Median Ratio	Log_2(Mutant/WT)	# of Peptide IDs
YLR314C	CDC3	0.78	-0.37	29
YJR076C	CDC11	0.81	-0.30	14
YDL225W	SHS1	0.86	-0.22	20
YJR092W	BUD4	1.03	0.05	11
YGL086W	MAD1	2.10	1.07	8
YKR095W	MLP1	1.83	0.87	87
YIL149C	MLP2	1.55	0.64	75
YJL041W	NSP1	1.65	0.72	12
YOR098C	NUP1	5.25	2.39	6
YLR335W	NUP2	1.10	0.13	18
YAR002W	NUP60	1.21	0.28	7
YPR010C	RPA135	1.74	0.80	8
YOR341W	RPA190	1.54	0.62	22
YOR340C	RPA43	0.96	-0.05	9
YOR295W	UAF30	2.28	1.19	6
YBR049C	REB1	1.11	0.15	47
YJL140W	RPB4	0.40	-1.34	10
YDL140C	RPO21	0.86	-0.22	60
YBR198C	TAF5	0.95	-0.07	15
YDR145W	TAF12	0.63	-0.67	13
YOR194C	TOA1	0.52	-0.94	19
YGL151W	NUT1	1.69	0.76	5
YBR279W	PAF1	1.04	0.06	14
YPR133C	SPN1	0.45	-1.14	12

YML010W	SPT5	0.60	-0.74	67
YER148W	SPT15	1.00	0.00	10
YGR186W	TFG1	0.52	-0.94	51
YLR399C	BDF1	0.65	-0.62	31
YGR252W	GCN5	0.91	-0.14	24
YGL066W	SGF73	0.98	-0.04	10
YBR081C	SPT7	1.22	0.29	75
YKR025W	RPC37	0.47	-1.10	14
YDL150W	RPC53	0.59	-0.77	26
YPR190C	RPC82	0.61	-0.71	25
YOR207C	RET1	0.50	-1.00	30
YAL001C	TFC3	0.74	-0.44	58
YGR047C	TFC4	1.14	0.19	6
YNL039W	BDP1	0.43	-1.20	41
YDR362C	TFC6	0.55	-0.85	11
YOR110W	TFC7	0.51	-0.98	9
YGR246C	BRF1	0.57	-0.81	27
YOR113W	AZF1	1.18	0.24	22
YJR060W	CBF1	0.94	-0.09	8
YOR028C	CIN5	0.27	-1.91	11
YCR084C	TUP1	0.69	-0.53	57
YBR112C	CYC8	0.76	-0.39	25
YNL167C	SKO1	0.93	-0.11	32
YPL181W	CTI6	0.89	-0.18	16
YNL027W	CRZ1	0.83	-0.27	7
YIL036W	CST6	0.72	-0.48	8
YPL049C	DIG1	0.82	-0.28	11
YHR084W	STE12	0.91	-0.14	9
YBR083W	TEC1	1.31	0.38	19
YNL199C	GCR2	0.45	-1.16	8
YLR256W	HAP1	0.83	-0.27	23
YOR032C	HMS1	0.97	-0.04	6
YNL103W	MET4	0.37	-1.45	26
YDR176W	NGG1	0.92	-0.13	21
YBL066C	SEF1	1.95	0.97	9
YDR310C	SUM1	1.29	0.37	76
YER111C	SWI4	0.91	-0.14	21
YOR344C	TYE7	0.31	-1.69	13
YDR213W	UPC2	1.25	0.32	20
YIL056W	VHR1	2.07	1.05	8
YER064C	YER064C	0.70	-0.51	18

YOR230W	WTM1	1.30	0.38	10
YPL228W	CET1	0.38	-1.39	41
YAL032C	PRP45	2.53	1.34	19
YMR229C	RRP5	2.02	1.01	28
YDR464W	SPP41	1.23	0.30	122
YDR169C	STB3	0.96	-0.06	25
YOR038C	HIR2	2.01	1.01	29
YBR215W	HPC2	1.65	0.72	39
YDR174W	HMO1	2.65	1.40	12
YBR245C	ISW1	1.02	0.02	61
YOR304W	ISW2	1.09	0.13	5
YML069W	POB3	0.84	-0.26	21
YOL004W	SIN3	1.00	0.00	39
YDR359C	VID21	0.97	-0.04	39
YGR056W	RSC1	1.01	0.02	38
YLR357W	RSC2	1.03	0.04	82
YFR037C	RSC8	0.69	-0.54	36
YLR033W	RSC58	0.76	-0.39	30
YMR091C	NPL6	0.72	-0.48	10
YIL126W	STH1	0.90	-0.15	60
YGR275W	RTT102	0.90	-0.14	6
YDR190C	RVB1	0.60	-0.74	11
YPL235W	RVB2	0.64	-0.63	8
YOR290C	SNF2	1.27	0.34	36
YBR289W	SNF5	0.78	-0.36	13
YJL176C	SWI3	0.74	-0.44	28
YDR334W	SWR1	1.08	0.11	44
YAL011W	SWC3	0.81	-0.30	34
YDR485C	VPS72	0.84	-0.25	41
YDL197C	ASF2	0.48	-1.07	17
YKL172W	EBP2	0.79	-0.34	16
YDR110W	FOB1	1.04	0.05	20
YNL132W	KRE33	2.97	1.57	9
YFR028C	CDC14	9.58	3.26	28
YJL076W	NET1	5.30	2.41	147
YNL216W	RAP1	1.07	0.10	49
YBR275C	RIF1	1.06	0.09	9
YLR442C	SIR3	1.20	0.27	38
YDR227W	SIR4	0.91	-0.14	91
YKR010C	TOF2	1.42	0.51	33
YFL008W	SMC1	1.83	0.87	17

YJL074C	SMC3	1.35	0.43	17
YDL003W	MCD1	1.07	0.10	11
YFR031C	SMC2	0.64	-0.64	22
YLR086W	SMC4	0.52	-0.95	41
YBL097W	BRN1	0.41	-1.30	27
YOL034W	SMC5	1.72	0.78	33
YLR383W	SMC6	2.10	1.07	21
YJR089W	BIR1	0.70	-0.52	67
YGR140W	CBF2	0.87	-0.20	36
YBR156C	SLI15	0.48	-1.07	51
YKL112W	ABF1	1.31	0.39	38
YLL004W	ORC3	1.55	0.64	13
YGL201C	MCM6	1.23	0.29	13
YBR088C	POL30	0.61	-0.71	18
YOL006C	TOP1	0.95	-0.07	38
YNL088W	TOP2	0.87	-0.20	47
YAL027W	YAL027W	1.05	0.07	8
YBR114W	RAD16	0.90	-0.15	35
YPR180W	AOS1	1.13	0.17	11
YDR390C	UBA2	1.40	0.49	23
YDL064W	UBC9	1.12	0.16	15
YDR409W	SIZ1	1.05	0.07	23
YOR156C	NFI1	0.76	-0.40	16
YNL042W	BOP3	1.99	0.99	32
YDL126C	CDC48	0.69	-0.54	37
YDR385W	EFT2	0.84	-0.24	25
YGR254W	ENO1	1.09	0.13	11
YLL026W	HSP104	1.62	0.69	5
YKL142W	MRP8	2.60	1.38	12
YOL070C	YOL070C	0.49	-1.02	6
YLR044C	PDC1	0.98	-0.03	21
YCR012W	PGK1	1.21	0.27	25
YOR191W	RIS1	0.47	-1.10	16
YER120W	SCS2	1.75	0.81	5
YLR354C	TAL1	1.02	0.03	8
YJL138C	TIF2	0.75	-0.42	22
YPR074C	TKL1	1.19	0.25	5
YMR111C	YMR111C	1.16	0.21	52
YBL023C	MCM2	2.29	1.19	6
YEL032W	MCM3	2.22	1.15	12

Supplementary Table 5. The median abundance ratios of the peptides derived from the SILAC SUMO proteomic experiment comparing HZY3983 (light media) and HZY 2101 (heavy media). A minimum requirement of 5 peptides IDs was used to filter the results.

Light: 3983 Heavy: 2101				
ORF	Gene	Median Ratio	Log$_2$(Mutant/WT)	# of Peptide IDs
YLR314C	CDC3	1.03	0.04	8
YKR095W	MLP1	0.59	-0.75	13
YIL149C	MLP2	0.78	-0.36	7
YBR049C	REB1	0.32	-1.65	14
YML010W	SPT5	1.00	0.00	11
YER148W	SPT15	2.47	1.31	5
YGR186W	TFG1	0.30	-1.72	21
YGR252W	GCN5	0.17	-2.55	7
YBR081C	SPT7	0.41	-1.29	7
YKR025W	RPC37	1.65	0.72	5
YDL150W	RPC53	1.64	0.72	9
YAL001C	TFC3	1.34	0.42	6
YNL039W	BDP1	2.78	1.48	15
YOR028C	CIN5	0.23	-2.13	5
YCR084C	TUP1	0.39	-1.37	19
YNL167C	SKO1	0.02	-5.66	5
YDR310C	SUM1	0.55	-0.87	7
YOR344C	TYE7	1.01	0.01	5
YPL228W	CET1	0.14	-2.81	6
YDR464W	SPP41	0.73	-0.45	38
YDR169C	STB3	0.06	-3.98	11
YBR215W	HPC2	0.07	-3.92	10
YDR359C	VID21	0.30	-1.74	5
YLR357W	RSC2	0.35	-1.53	7
YFR037C	RSC8	0.58	-0.78	8
YAL011W	SWC3	0.19	-2.41	7
YDR485C	VPS72	0.14	-2.80	11
YDR110W	FOB1	1.41	0.49	6
YFR028C	CDC14	35.18	5.14	12
YJL076W	NET1	20.00	4.32	99
YNL216W	RAP1	0.34	-1.56	13
YDR227W	SIR4	0.45	-1.16	25

YKR010C	TOF2	6.93	2.79	14
YBL097W	BRN1	0.95	-0.07	5
YJR089W	BIR1	0.96	-0.05	16
YGR140W	CBF2	3.23	1.69	5
YBR156C	SLI15	0.91	-0.13	5
YKL112W	ABF1	0.28	-1.85	13
YBR088C	POL30	0.52	-0.95	9
YDR390C	UBA2	0.80	-0.32	7
YDL064W	UBC9	0.28	-1.82	6
YDR409W	SIZ1	0.45	-1.15	6
YNL042W	BOP3	0.12	-3.08	14
YDL126C	CDC48	4.83	2.27	21
YLR044C	PDC1	1.16	0.22	5
YCR012W	PGK1	0.56	-0.84	12